The Drop-size Distributions in Well-developed Convective Rainclouds: Part 1

Characteristic features of size distribution observed during a thunderstorm on July 13, 1969

By Yoshiharu SHIOTSUKI

(Dep. of Civil Engineering, Technical Junior College of Yamaguchi University,)

Abstract

Simultaneous work of the raindrop sampling and the radar observation was made in heavy rainfalls during the last stages of Baiu at Histoyoshi in southern Kyushu. The equation for the drop-size distribution was obtained in such well developed convective rainfalls in the form of $N_D = N_0 e^{-\Lambda D^2}$ ($N_0 = 200$, $\Lambda = 1.2\ R^{-0.5}$, R: mm/hr, D: mm) at the drop size range larger than 1 mm diameter. And it is quite similar to the stationary distribution computed by Srivastava[19]. This paper involves some considerations on the new obtained size spectra and rain parameters derived from it, and suggests that a combination effect of several different raincells may also be responsible for the new type distribution, in addition to the various kinds of cloud physical effects. The results of numerical experiments in relation to the observed characteristic distribution will be described in Part 2 of this paper.

1. Introduction

The size distributions of raindrops in various types of rains have been studied by many investigators. The studies were carried out mainly for radar measurement of rainfall amount, and for the cloud dynamic studies on the difference of size distributions directly related to the growth process of raindrops. Marshall and Palmer[13] first proposed the well known empirical formula of exponential type for the size distribution of raindrops, namely the M–P equation. Because this equation is simple in form and is highly applicable in the theoretical treatment of various types of rain parameters, it is frequently utilized to give standard size distributions of raindrops. Many investigators after Marshall and Palmer have made observations of size distribution of raindrops, and it has become accepted that the M–P equation and the derived rain parameters, for example, the Z–R relationship where $Z = 200\,R^{1.6}$ were quite adequate for practical purposes.

The M–P equation, however, is obtained by smoothing out the size distribution of raindrops of stratiform rains. Therefore the equation may not be applicable in the case of heavy convective rains. Further in the equation, the space concentration of raindrops is over-estimated, especially in the region of raindrops smaller than 1.5 mm in diameter. Best[3] examined the resulting

discrepancies in the determination of the size distribution by the M–P equation, and presented a modified formula. Although these equations often give a fairly good approximation of the average size distribution in continuous or homogeneous stratiform rain, it is frequently noted that the distribution of raindrops, sampled in periods of only a few minutes in a shower and even a continuous warm frontal rain, show considerable deviation from the average (Mason and Ramanadham,[16] Mason and Andrews,[15] Dingle and Hardy[6]). Hence taking into consideration the departures from the average distibutions, recently studies with the aid of a computer have been made to evaluate the effects of coalescence with other drops, accretion of cloud droplets, and evaporation of drops. (e.g., Mason and Ramanahdam,[16] Rigby[17], et al, Hardy[9]). Srivastava[19] studied the effect of breakup and coalescence using a computer. And now, for the development of doppler-radar system, the drop size distribution still remains a problematic point.

The present writer investigated heavy rainfalls in Kyushu during the terminal stages of Baiu, utilizing the PPI and RHI weather radar, covering a period of several years. The present paper describes the characteristic properties of size distibution of raindrops in heavy rainfalls. The rainfalls here were associated with thunderstorms which precipitated very large raindrops on the ground surface. More than 20,000 raindrops were sampled simultaneously in the radar observation. A theoretical consideration on such characteristics as size distributions will be reported in Part 2 and Part 3 of this paper.

2. Measurement of raindrops

The size distribution of raindrops was measured by the filter paper method. The surface area of filter paper was 250 cm^2, however the distribution in the central portion was used in order to avoid side effects on the true distribution.

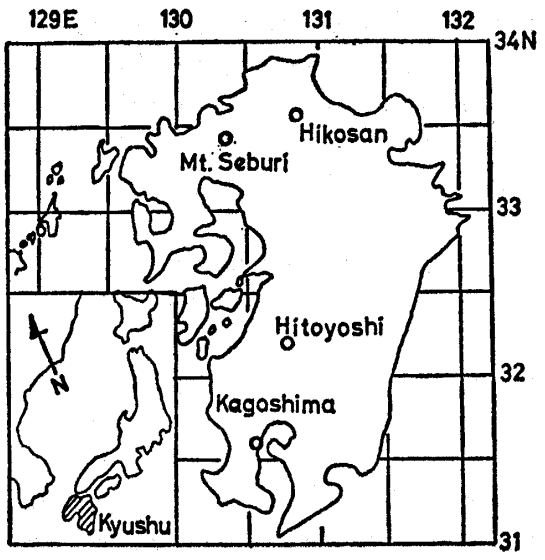

Fig. 1 Local map of Kyushu.

This 100 cm^2 portion seems small when compared with the sampling area used hitherto by researchers, for instance, in the case of Blanchard[4], it was 252 cm^2. But the present 100 cm^2 was used for the following reason.

In the case of a heavy rainfall, the exposure time must be quite short, for instance, 1 second. In such a short time, it was very difficult to give the entire surface area of the filter paper an accurate uniform exposure, in addition the data at the periphery of the paper would not be correct. The drawbacks due to a lesser sampling area was compensated for by repeated sampling every 15–60 seconds. The diameter of spots on the filter paper were read at 1 mm intervals. This interval corresponds to about a 0.2 mm interval for raindrops smaller than 1.0 mm in diameter, about a 0.15 mm interval for drops from 1.0 to 2.5 mm, and about a 0.1 mm interval for drops larger than 2.5 mm. The

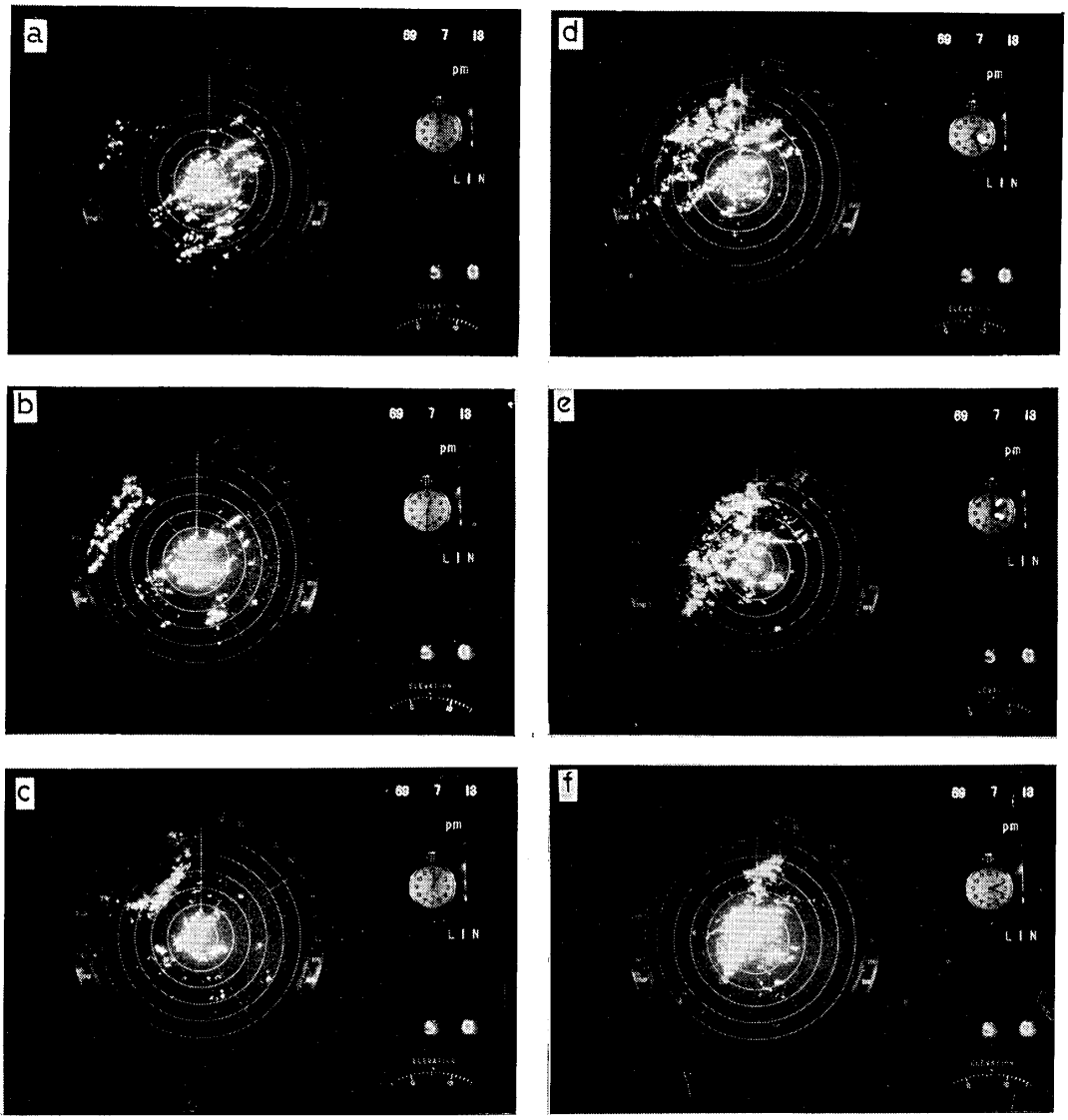

Fig. 2 Time change of PPI display of two line echoes on July 13, 1969. (a) 1200 JST (b) 1230 (c) 1300 (d) 1325 (e) 1400 (f) 1418. 10 km range markers and elevation angle 5~6 deg.

size distribution was described in these intervals as given above. Therefore the plotting of the larger drops was denser than the smaller drops in the description of size distribution.

The raindrop measurements and the radar observations in heavy rainfalls were made at Hitoyoshi in southern Kyushu, as shown in Fig. 1. The weather radar used has a 3.2 cm wave length, a peak power of 60 kw, a pulse length of 1.5 μs, a conical beam width of 1.0°, and a maximum range of 100 km. And it also can given both displays of PPI and RHI with the iso-echo contouring in a range of 60 km.

Raindrop data in the present paper were obtained from ten individual rainfalls associated with the passage of a cold frontal thunder-storm in the afternoon of July, 13, 1969. Fig. 2 shows the general features of PPI echoes at 1200–1420 JST. In the figure two line type echoes are seen. One is associated with a cold front moving from the north-west, and the other is a stationary one with an orientation bearing from south-west to north-east near Hitoyoshi. These two line echoes coalesced at 1400 JST after which the coalesced echoes rapidly increased their radar reflectivity moving towards the south-east. The rainfalls from these echoes began at the radar site at 1442 JST.

Fig. 3 shows the time change of the rainfall rates and the observed maximum drop diameter at every 30 or 60 seconds, for a period of about two and a half hours, before and after the passage of cold frontal line echoes. As pointed out by Dingle and Hardy[6] in a cold frontal shower, a high rainfall intensity accompanying large drops are frequently seen during the beginning few minutes

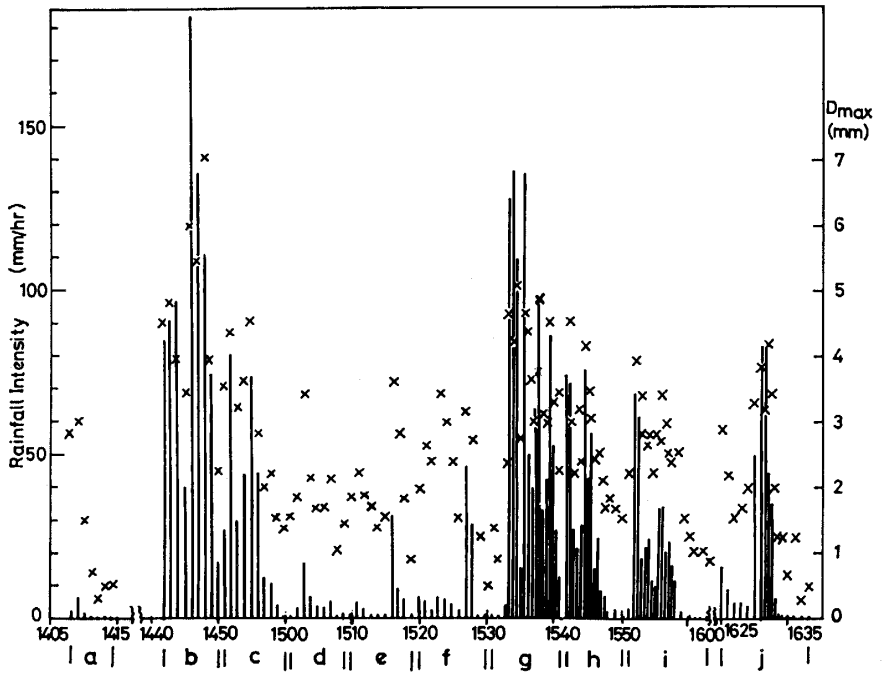

Fig. 3 Time change of the rainfall intensity and the maximum diameter of raindrops, obtained in each instantaneous sample.

in the case of high intensity rainfall. Correspondence between the rainfall intensity and the maximum diameter of drops is very good.

3. Raindrop size distributions

a) Instantaneous size distributions

Typical examples of instantaneous size distributions of raindrops according to variation of rainfall rates are exhibited in Fig. 4. These were taken in about one second exposures. As seen in the figure, when the rainfall intensity becomes higher to a certain extent, the plots do not appear in the M–P type distributions, in such a manner that the increased space distributions of both the small and large drops and the dip of medium size appear in the corresponding M–P distributions. A similar tendency was already noted and considered by Mason and Andrews,[15] and Dingle and Hardy.[6] The former explained that the increment of large drops may be caused by a coalescence growth process of drops, and a large number of small drops by splashing which appeared as large drops colliding with the surface. And in addition the latter suggested that the small drops in excess is due to the aerodynamic breakup of large drops occuring during their fall, and on the large drop increment they asserted that the sorting effect

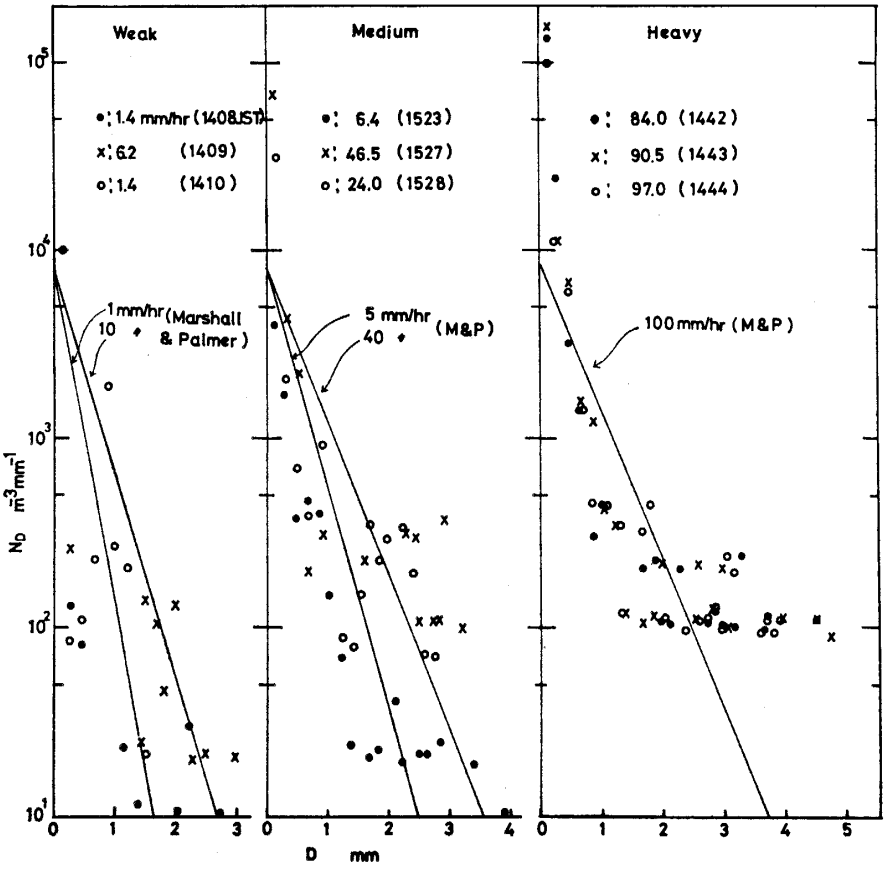

Fig. 4 Examples of instantaneous size distribution of raindrops.

of gravity and wind shear was involved. On the other hand, in the case of the present rainfalls reported here, the appearance of those different distributions from the M–P equation is not always limited to the early stages of the rainfall, but it was also found during the last stages of rainfall, for instance, as shown in the plots of 1528 JST in Fig. 4.

Thus the coalescence process may be highly responsible for the excess of space concentrations of large drops. However, our instantaneous sampling volume was never large enough when compared with the statistical criterion by Joss and Waldvogel,[11] and the obtained size distributions appeared usually to be discrete, hence further discussions could not be made on the problems of the growth process of raindrops. But such characteristic distributions will be discussed again in Part 2 and Part 3, and described as highly possible distributions which may be expected from theoretical studies. Next, the average size distributions for each rainfall will be dealt with.

b) Average size distributions of each rainfall

Average size distributions for each rainfall, in which the continuation time is about 10 minutes as shown in Fig. 3, were obtained by averaging the total of instantaneous distributions in each shower. Fig. 5 represents these average size distributions for each rainfall with the RHI displays of their mother convective echoes.

Generally it is said that the movement of convective cell echoes are in good agreement with the upper wind between 700 and 600 mb (Tatehira[21]). While the upper wind data at Kagoshima at 1500 JST on this day revealed this level wind by WSW 40 kts, the actual moving speed of the cell was about 50 or 60 km/hr on the radar scope. This speed corresponds well to the 10 minute continuation time of one rainfall because the size of the convective cell was usually about 10 km in diameter. In the figure, the displays of the iso-echo contour in RHI are also shown for each rainfall of 1442–1450 JST and 1531–1541 JST of which intensities were high. In these, ISO 4, 5, 6 and 7 correspond to the radar reflectivities $Z=6.3\cdot10^2$, $1.8\cdot10^3$, $5.5\cdot10^3$, $1.7\cdot10^4$ in mm^6/m^3, respectively. Generally, we can find a high reflectivity in the leading edge or the downwind-side of the cell. This corresponds well to that of numerous large raindrops which were often observed at the beginning of each rainfall.

Now it can be seen that the average distributions of each rainfall in Fig. 5 also remain to show the dips from the corresponding M–P equation in a medium size region, except for the weak rainfall of 1501–1508 JST. These dips appear remarkably in the cases of rainfalls of high intensity, 1442–1450, 1531–1541 JST, in such a way that excess values were seen in space concentrations of drops in a range of small size ($D\leqq1.0$ mm) and large size ($D\geqq3$ mm), while on the other hand least values were seen in a size range falling between the two extremes where the distributions tend to be flatter. Such flatter distributions appear again in a range of drop size larger than 4 mm, but the values were rather discrete. The distribution profiles in these high intensity rainfalls, therefore,

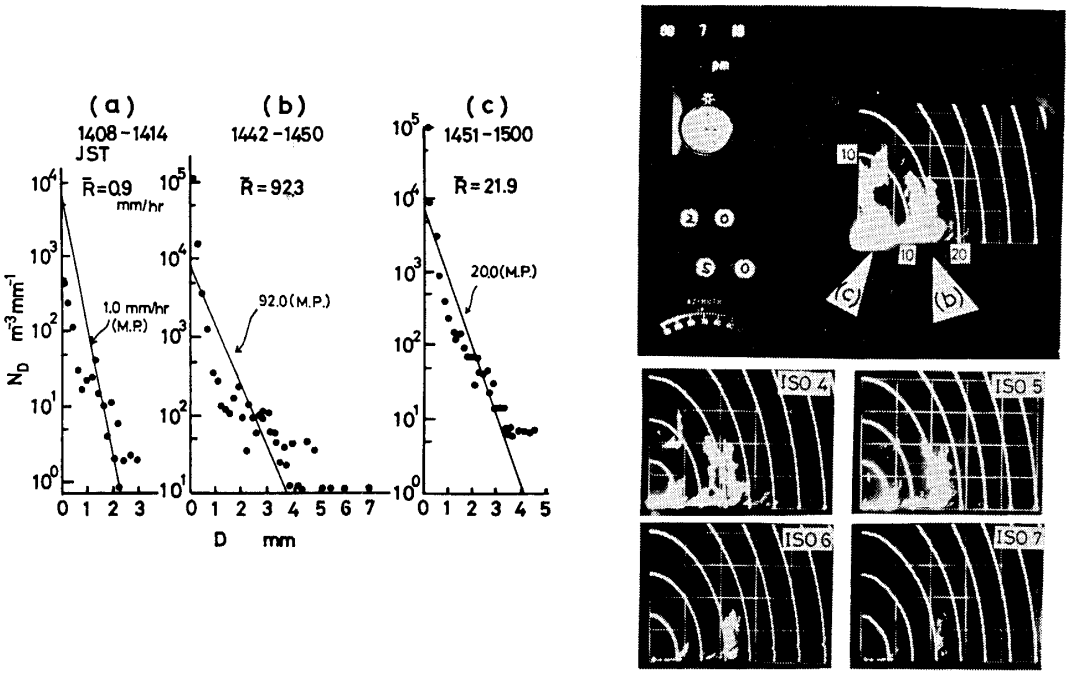
(a)
1408-1414
JST
R̄=0.9
mm/hr
1.0 mm/hr
(M.P.)
(b)
1442-1450
R̄=92.3
92.0(M.P.)
(c)
1451-1500
R̄=21.9
20.0(M.P.)
N_D m^-3 mm^-1
D mm
ISO 4
ISO 5
ISO 6
ISO 7

Fig. 5—1

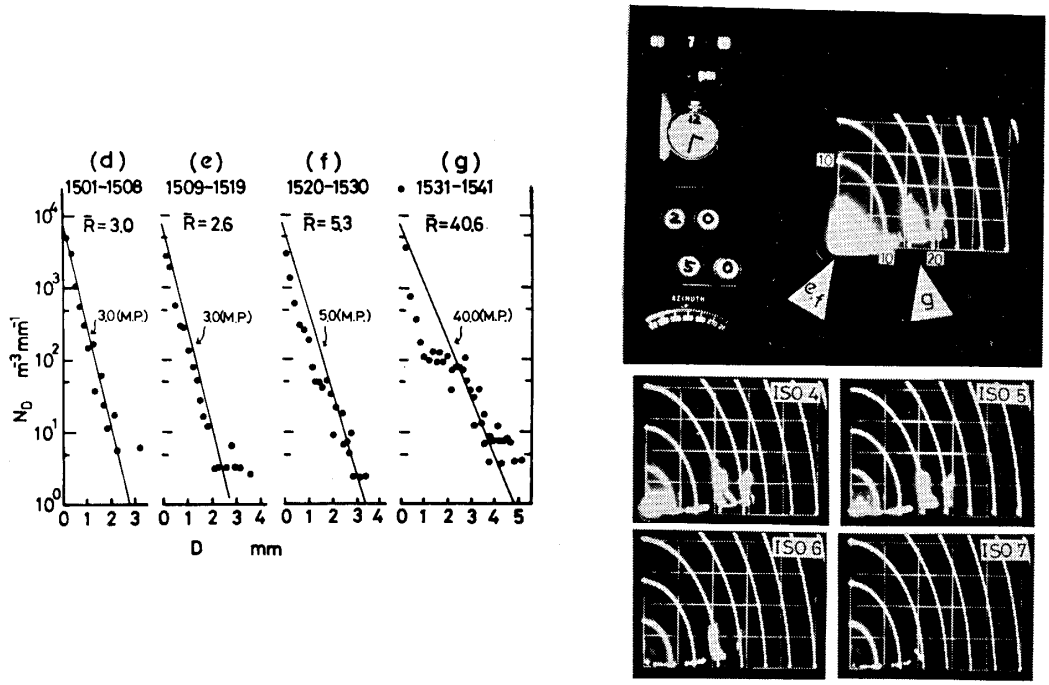
(d)
1501-1508
R̄=3.0
3.0(M.P.)
(e)
1509-1519
R̄=2.6
3.0(M.P.)
(f)
1520-1530
R̄=5.3
5.0(M.P.)
(g)
1531-1541
R̄=40.6
40.0(M.P.)
N_D m^-3 mm^-1
D mm
ISO 4
ISO 5
ISO 6
ISO 7

Fig. 5—2

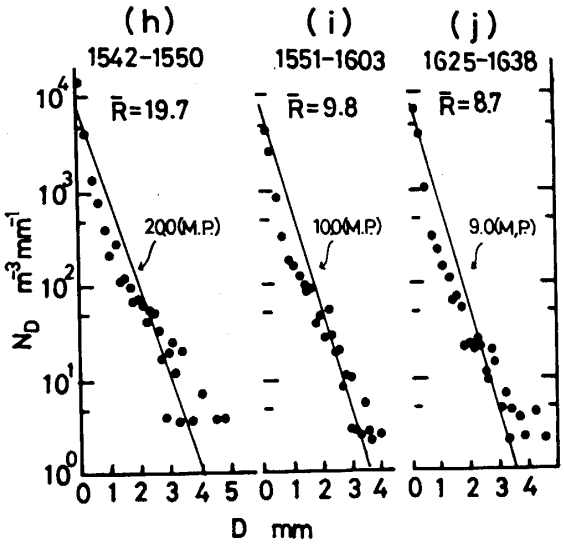

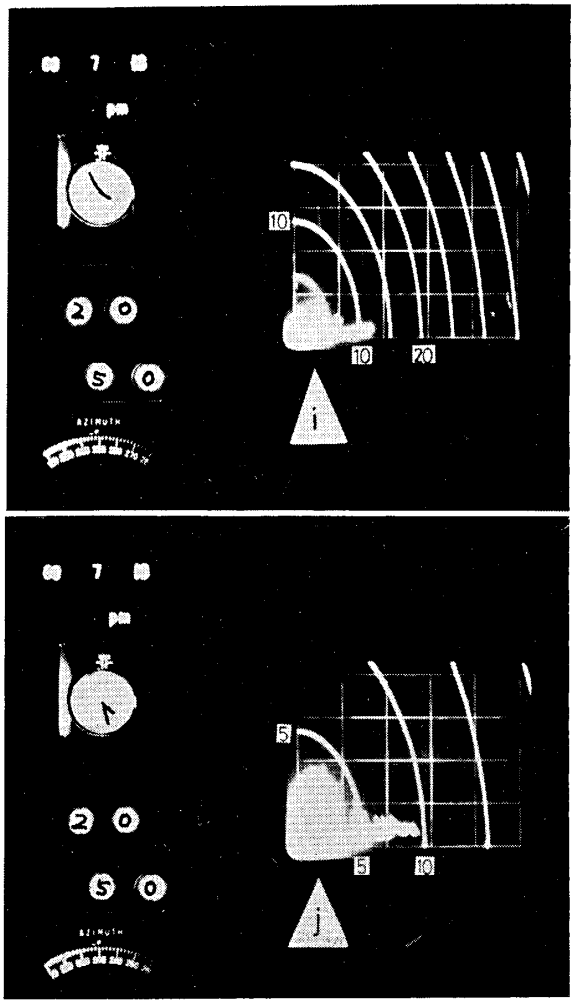

Fig. 5 Average size distributions for each rainfall, (a)–(j) in Fig. 3, and the RHI displays of their mother rainclouds. Distribution curves of the Marshall-Palmer (M. P.) are also drawn in the figure, corresponding to the observed mean intensity of each rainfall.

Fig. 5—3

reveal themselves as step-changed forms. Moreover it is interesting to note that the space concentration at a drop diameter 0.15 mm is in excess of $N_D=10^4$ $m^{-3}mm^{-1}$ in the case of rainfall rates which exceed approximately 20 $mm\cdot hr^{-1}$. Especially it was noted that a development of more than 10^5 $m^{-3}mm^{-1}$ in the rainfalls during 1442–1450, 1451–1500 JST were seen with regards to this, RHI displays show the echo height reaching to about 10 km. These high developed clouds increase the falling distance of involved raindrops and may progressively cause the effects of coalescence, breakup and splash. In addition to these effects, recently Srivastava[19] suggested the effect of drop disintegration on collision from the results of his numerical experiments in which the breakup effect could not attain the observed space concentrations of small drops.

On the other hand, Blanchard[4] obtained more than 10^5 $m^{-3}mm^{-1}$ of space concentrations of small drops ($D\sim0.1$ mm) in Hawaiian orographic warm rain. Also in Kyushu we can often find warm rain cloud in the lower layer of the atmosphere in summer. Thus small drops grown in these warm rain clouds may also be taken into account when high concentrations of small drops are considered in the event that they are transported to the surface by the downdraft current caused by the falling of large drops from high developed rain clouds.

c) Parabolic size distributions on the semi-logarithmic paper

As shown in Fig. 5, our size distributions from the heavy rainfalls can not be represented by a simple function of drop size D, and the plots still remain a little discrete in a range of large drops even in the average distributions. For statistical treatment, again the N_D values in each rainfall of Fig. 5 were averaged at every 0.5 mm interval of drop diameter.

At first, these representative values of N_D were plotted in both-logarithmic graph papers to see where the size range occupies the most space liquid water content (*L.W.C.*) as shown in Fig. 6. The solid lines in the figure show the distributed amount of *L.W.C.* to a certain size of drop, if *L.W.C.* were equally divided to distribute to any size of drop diamter. These are calculated as follows by giving the maximum diameter of drops. If an ideal distribution $N_D=AD^{-3}$ (A: constant) is considered in $L.W.C.=\int_0^{D_{max}}\frac{\pi}{6}\cdot\rho\cdot N_D\cdot D^3\,dD$, the coefficient A will be obtained as $A=6\cdot10^3\cdot L.W.C./(D_{max}\cdot\pi)$. In Fig. 6 the observed maximum diameter 7 mm was used for D_{max}. (Explanations on this ideal distribution in increased detail will be made in Part 3 of this report.) In the figure, also the M–P distributions are replotted by the dotted lines. Generally it is seen that the concentration of *L.W.C.* of the present distributions appear in the larger size range of drop diameter compared with the M–P family. And they might be fitted by linear regression curves such as $N_D=AD^{-\alpha}$ (A, α: constant) or parabolic $N_D=B\exp\{-\beta(ln\gamma D)^2\}$ (B, β, γ: constant). And they should give a good representation of the size distributions expected to be removed according to their rain intensity. In fact, the expected values of certain types of rain parameters by both regression curves give a good approximation of the observed,

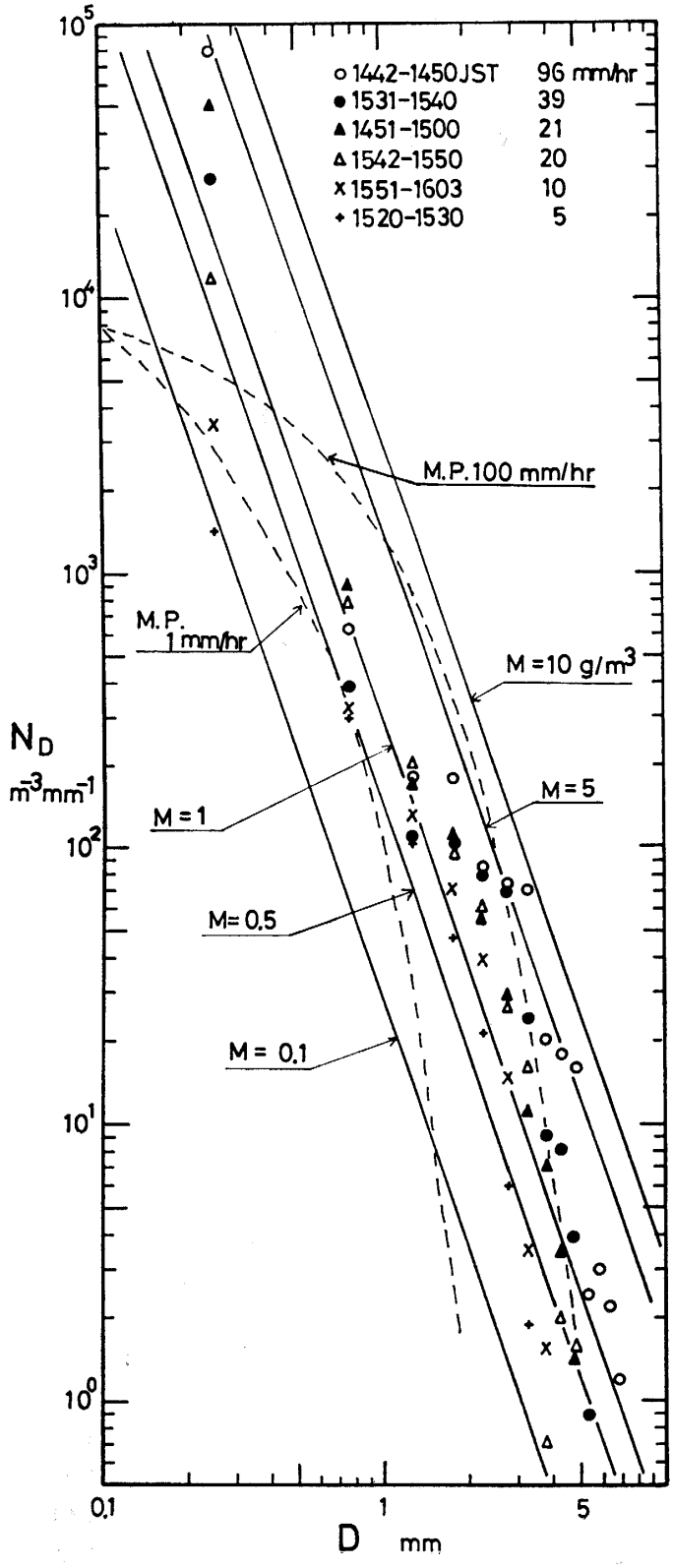

Fig. 6 Drop-size spectra of each rainfall in Fig. 5 on both-logarithmic graph paper. N_D values here averaged at every 0.5 mm interval of drop diameter. Solid lines indicate the "ideal distribution" by which liquid water content may be equally divided to distribute to any size of drop diameter. Dotted lines show the M–P distribution.

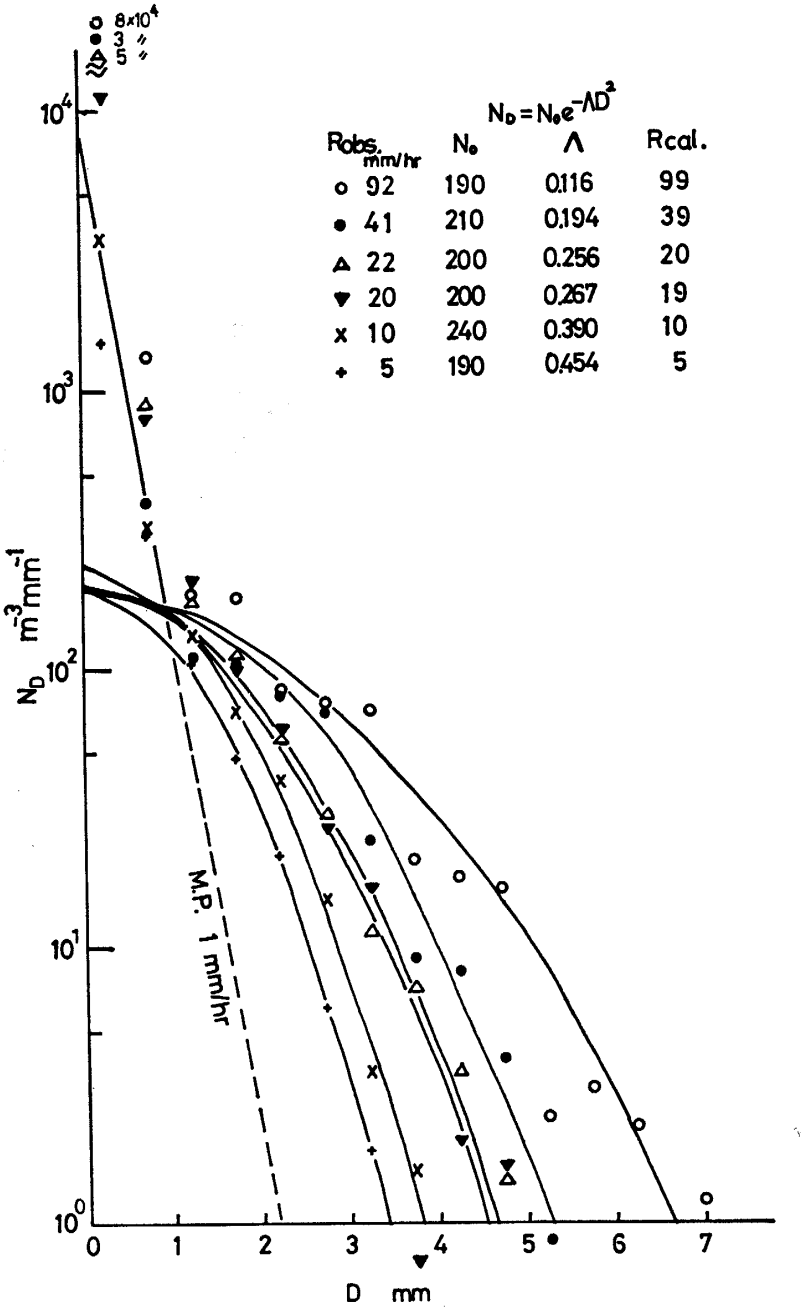

Fig. 7 Drop-size spectra of each rainfall in Fig. 6 fitted by parabolic curve. Robs, Zobs and Rcal, Zcal indicate the R, Z values of both observed and calculated by the parabolic equation, respectively.

say, within a margin of $\pm 10\%$. But the former needs a value of maximum diameter which is ordinarily less representative than a median volume diameter. And the reflectivity factor calculated by the latter form was always larger by one order than the observed when infinity was adopted instead of D_{max}. Therefore, the distributions were fitted by the parabolic regression curve on the same coordinates as the M–P distributions as shown in Fig. 7. The new fitted distribution function $N_D = N_0 \exp(-\Lambda D^2)$ (N, Λ: constant) gives a good representation of the hill of the spectrum in a medium size range and another abrupt decrement of drop population in the larger size. Where the fitting of curves were made within the size range over 1 mm in diameter, because the drops below 1 mm will contribute but little to any of the rain parameters, as far as a rainfall of high intensity is concerned. In the figure, the values of the coefficients N_0 (space drop concentration at $D=0$ mm) and Λ are shown with the observed and calculated values of R and Z. A good agreement between the observed and the calculated values from the determined distribution function are seen except for the value of Z of the 1442–1450 rainfall. The values of Λ seem to decrease in accordance with rainfall rate, while the values of N_0 are rather fixed to the constant, at about 200 $m^{-3}mm^{-1}$. Fig. 8 shows the correlation between the coefficient Λ and R which is more than 10 mm/hr. From the figure $\Lambda = 1.2\, R^{-0.5}$ is obtained. Thus the size distribution curves of the present developed convective rainfalls may be illustrated in Fig. 9, and compared with the M–P family. The overall profile of size distribution would be accomplished by adding to them the M–P 1 mm/hr distribution of which contribution to the rain parameters is quite less.

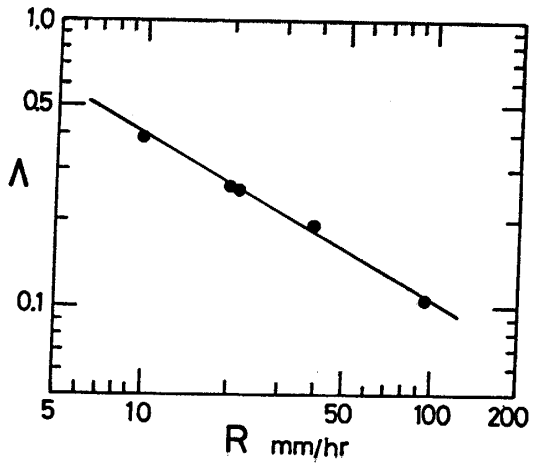

Fig. 8 Correlation between Λ and R.

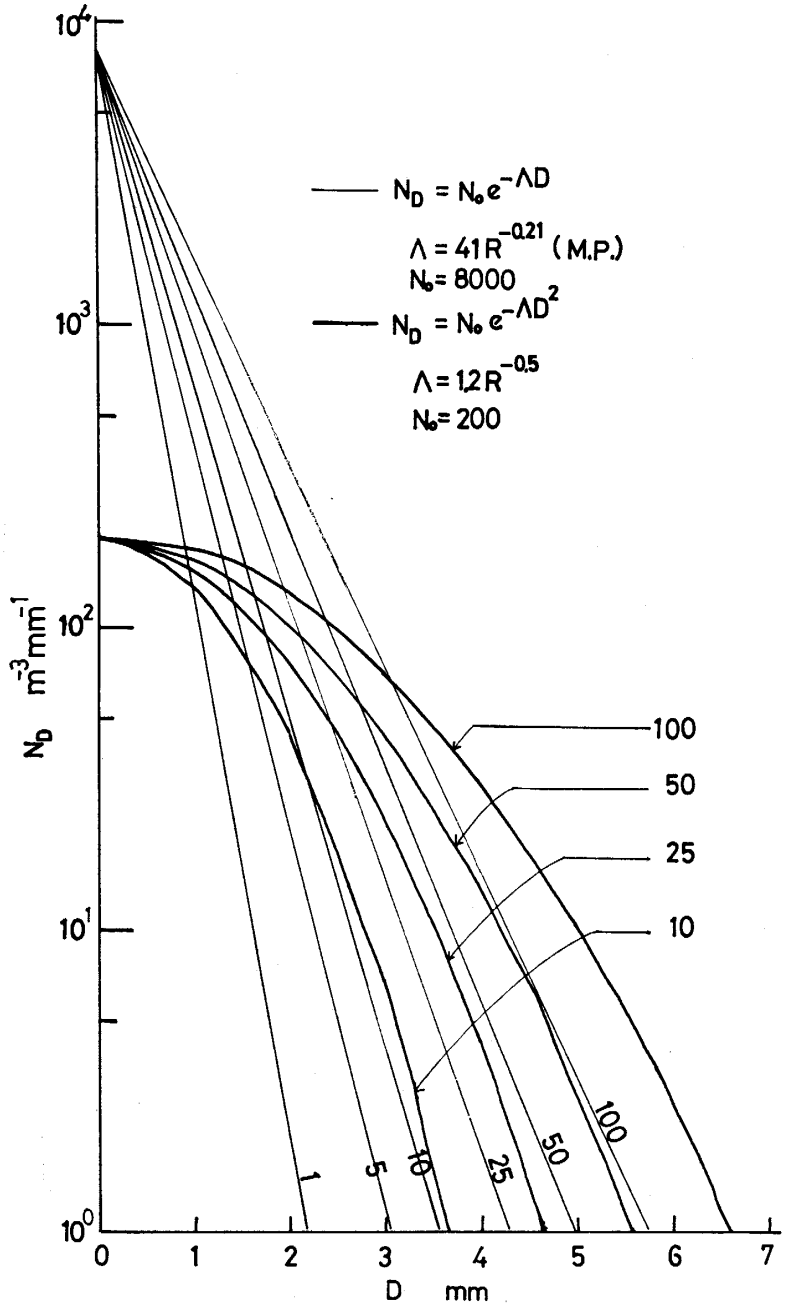

Fig. 9 Comparison of the M-P and the present distributions.

d) Rain parameters

The main four rain parameters R (rain intensity, mm/hr), Z (reflectivity factor, mm^6/m^3), *L.W.C.* (liquid water content, g/m^3) and D_0 (median volume diameter, mm) can be calculated by the following equations.

$$N_D = N_0 \exp\{-\Lambda D^2\}$$

$$R = \int_0^\infty \frac{\pi}{6} \cdot \rho \cdot N_D \cdot v \cdot D^3 dD$$

$$= \frac{\pi}{6} \cdot \rho \cdot N_0 \cdot k \cdot \Gamma\left(3+\frac{n}{2}\right) / \{A^{2+\frac{n}{2}}(4+n)\}$$

$$Z = \int_0^\infty N_D D^6 dD$$

$$= N_0 \cdot \Gamma(4.5)/(7\ A^{2.5})$$

$$L.W.C. = \int_0^\infty \frac{\pi}{6} \cdot \rho \cdot N_D \cdot D^3 dD$$

$$= \frac{\pi}{6} \cdot \rho \cdot N_D \cdot \Gamma(3)/4A^2$$

$$\frac{1}{2} L.W.C. = \int_0^{D_0} \frac{\pi}{6} \cdot \rho \cdot N_D \cdot D^3 dD$$

$$= \sum_{D=0}^{D_0} \frac{\pi}{6} \cdot \rho \cdot N_D \cdot D^3 \Delta D$$

, where ρ is the density of water, and k, n are constants of the velocity of drop by Gunn & Kinzer,[8] $v = kD^n$. Now we can obtain the relationship of Z–R, Z–$L.W.C.$ and R–$L.W.C.$ by eliminating A from each combined equation, when $A = 1.2\ R^{-0.5}$ is adopted. They are

$$Z = 383\ R^{1.6}$$
$$Z = 5.80 \cdot 10^4 L.W.C.^{1.75}$$
$$L.W.C. = 5.81 \cdot 10^{-2}\ R^{0.87}.$$

Atlas[1] summarized the characteristics of these main parameters from the various types of rainfall, and prepared a convenient rain parameter diagram. Mason[14] also collected and discussed the Z–R relationship obtained in various places over the world. And Fujiwara[7] noted the difference of Z–R relations between individual rainstorms. The comparison of the present parameters with the above results are made as follows. $Z = 383\ R^{1.6}$ appears to belong to the continuous rainfall families of Fujiwara's diagram, although the mother rain clouds were the developed convective type of thunderstorm. But in his schematic illustration of echo characteristics, the point of the values of 383 and 1.6 will generally be in the region of the completely diffused echo from a thunderstorm. In other relations of Z–$L.W.C.$ and $L.W.C.$–R, almost all of the values of parameters are larger than that of thunderstorm rain in Illinois ($L.W.C. = 5.2 \cdot 10^{-2}\ R^{0.97}$, $Z = 3.15 \cdot 10^4 L.W.C.^{1.41}$, Jones)[10], and in India ($L.W.C. = 7.0 \cdot 10^{-2}\ R^{0.83}$, $Z = 2.01 \cdot 10^4 L.W.C.^{1.70}$, Sivaramakrishnan)[18]. This may be because of the effects of abundant large size drops in the present case.

Atlas and Chmela[2] developed a useful rain parameter diagram by which we can determine the residual two parameters upon knowing two out of the four parameters, Z, R, $L.W.C.$ and D_0. The present data will make up for the upper-right part of this diagram as shown in Fig. 10. In the figure, the black circles indicate the plots of observed Z–R values in Fig. 7. and the broken

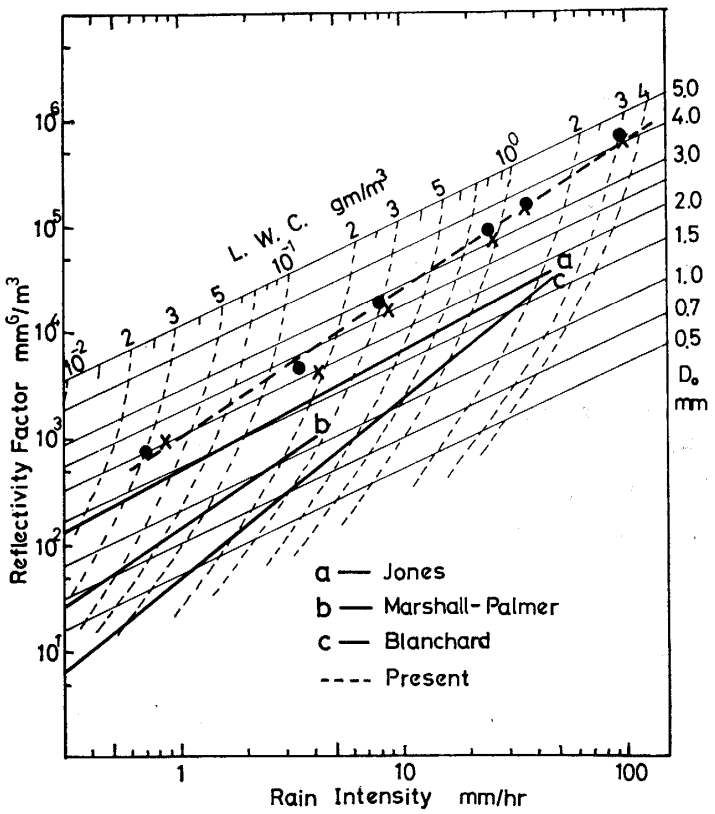

Fig. 10 Present data on the Rain Parameter Diagram after Atlas and Chmela (1957).

line shows the relationship of $Z=383\ R^{1.6}$. In the cases of high rainfall intensity, the values of D_0 and *L.W.C.* are slightly different in comparison with the expected values by the parameter diagram, such as $D_0=3.5$ (mm), *L.W.C.*$=3.3$ (g/m^3) at $R=96$ (mm/hr) rainfall, and $D_0=2.9$, *L.W.C.*$=1.5$ at $R=39$ rainfall, and $D_0=2.1$, *L.W.C.*$=0.9$ at $R=21$ rainfall, respectively. This may be because of the fact that the statistical parameters of G and $\bar{v}/v_0$ are different when compared with 1.5 and 0.98, respectively, which were adopted in Fig. 10 by Atlas and Chela. Atlas suggested that all the *Z–R* lines in this figure might converge between 20 and 50 mm/hr of rainfall rates, independent of the types of their rainfall. But our *Z–R* line does not obey this rule any more.

4. Considerations

It may be said that the raindrop size distributions from a sequence of highly developed convective rainfalls are of a new type which contain certain different characteristics of rain parameters as compared again to results of previous workers. Recently, Blanchard and Spencer[5] and Srivastava[19] obtained a similar distribution form as that reported at Hitoyoshi. The former authors studied the effect of drop breakup on a size distribution using an artificial rain column and suggested that in heavy rain the shape of the drop size dis-

tribution is determined by drop collision and breakup. The latter suthor followed this problem in the presence of the processes of drop breakup and coalescence using a stochastic equation, and conputed the stationary drop size distribution. The present distribution is quite similar to the stationary distribution obtained by him. Hence, it is considered that the average distribution at Hitoyoshi must have been remarkably influenced by the effects of drop breakup and coalescence in size range larger than 1 mm diameter.

One of most important results of Srivastava's computation is that the stationary distributions are roughly in parallel with each other. As shown in Fig. 6, the average distribution at Hitoyoshi tends to move almost in parallel in accordance with the change of the rainfall rate. The other is that, for a given water content, the stationary distribution is independent of the assumed initial distribution. This indicates that to what extent the space liquid water content is concentrated becomes a important problem for a heavy rainfall. Ludlum[12] indicated that the developed convective clouds consist of a great number of thermals. It may be admitted to extend this thought to the extent that the raindrop distributions within heavy rainfalls are composed of the raindrops which were produced in each individual thermal. A similar thought was applied in trying to explain the mechanism of severe storms by Bates[22]. Takeda[20] also noted the raindrops in the individual air parcels in an attempt to clarify the new generating points of updrafts.

It was described previously that the 1442–1450 JST rainfall was brought from cold frontal echoes which coalesced with two line type echoes; one was a moving cold frontal and the other was stationary in a warm region of a low. Fig. 11 shows the PPI displays of 3 levels of reflectivity immediately before (1400 JST) and immediately after (1410 JST) the two line echoes coalesced. It was found that the coalescence of echoes distinguished the increment of radar reflectivity. The size distributions from this coalesced echo (Fig. 5 (b)) show that the space concentrations of the medium size drops ($D=1\sim3$ mm) tend to rank along $N_D=10^2$ m^{-3}mm^{-1}, and the large drops ($D\geqq4$ mm) rank along $N_D=10$ m^{-3}mm^{-1}.

Such as coalescence of echoes were often seen on the radar scope in summer at Hitoyoshi. The two convective echoes in Fig. 5(g) (1531–1541 JST rainfall) were separate at first, but grew into one echo near the radar site as shown in Fig. 12. The size distribution from this echo is quite characteristic as well as 1442–1450 JST rainfall. Fig. 13 shows another example of the united echo. It may be seen from the figure that both echo types of convective and stratiform coexist in a large cell, and the precipiration from the latter which originated in the bright band coalesces with the convective at a 2 km height.

Incidentally, Fig. 14 shows the size distribution from a well developed convective rainfall associated with a winter low. These were observed in the afternoon on Jan. 21, 1971, at Hikosan (Fig. 1) during snow observations. Rainfall changed to snowfall in the morning of the following day. Mt. Seburi

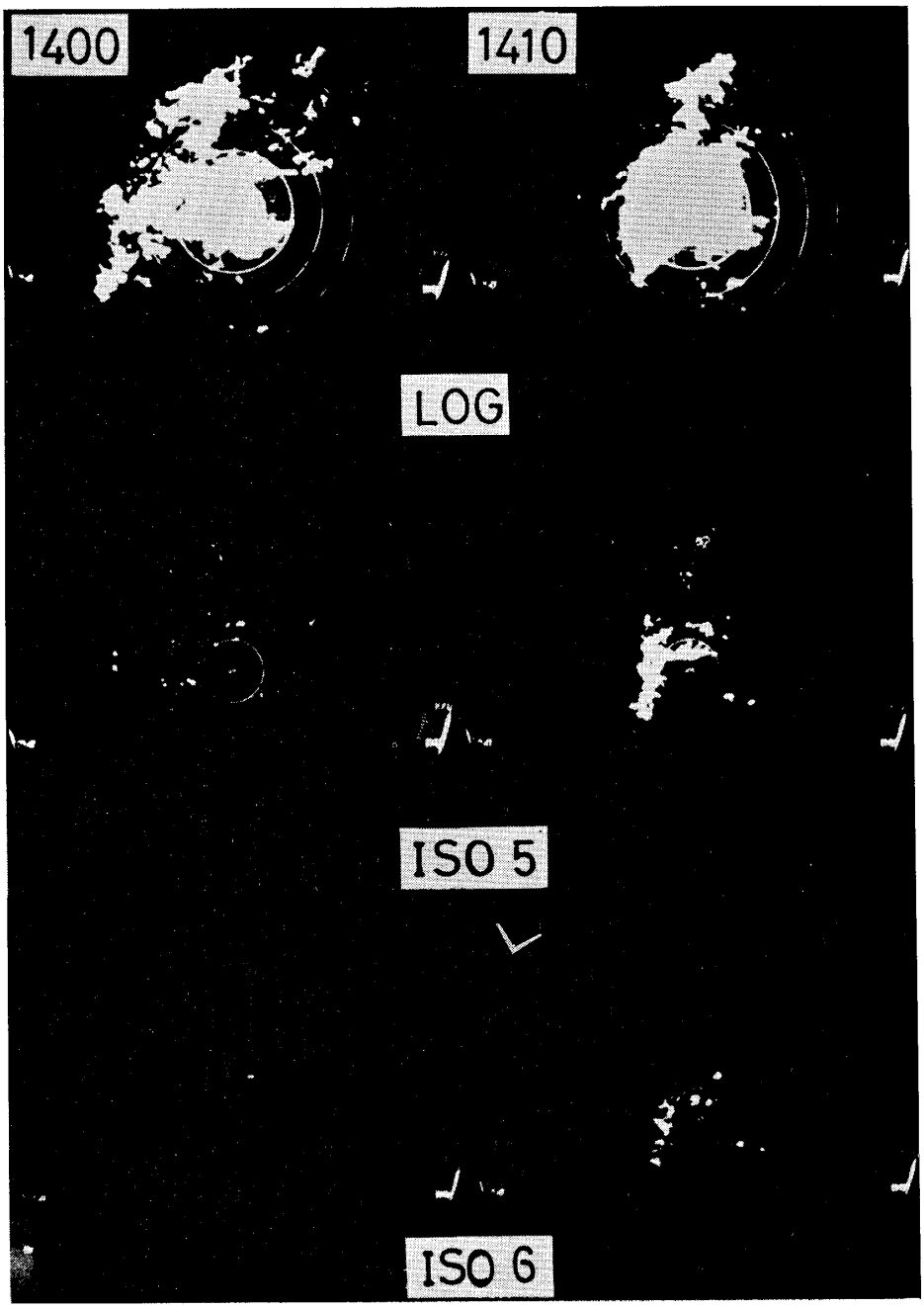

Fig. 11 The change of PPI displays of 3 levels of reflectivity when two line echoes coalesced. The coalesced echo brought the rainfall of Fig. 5 (b).

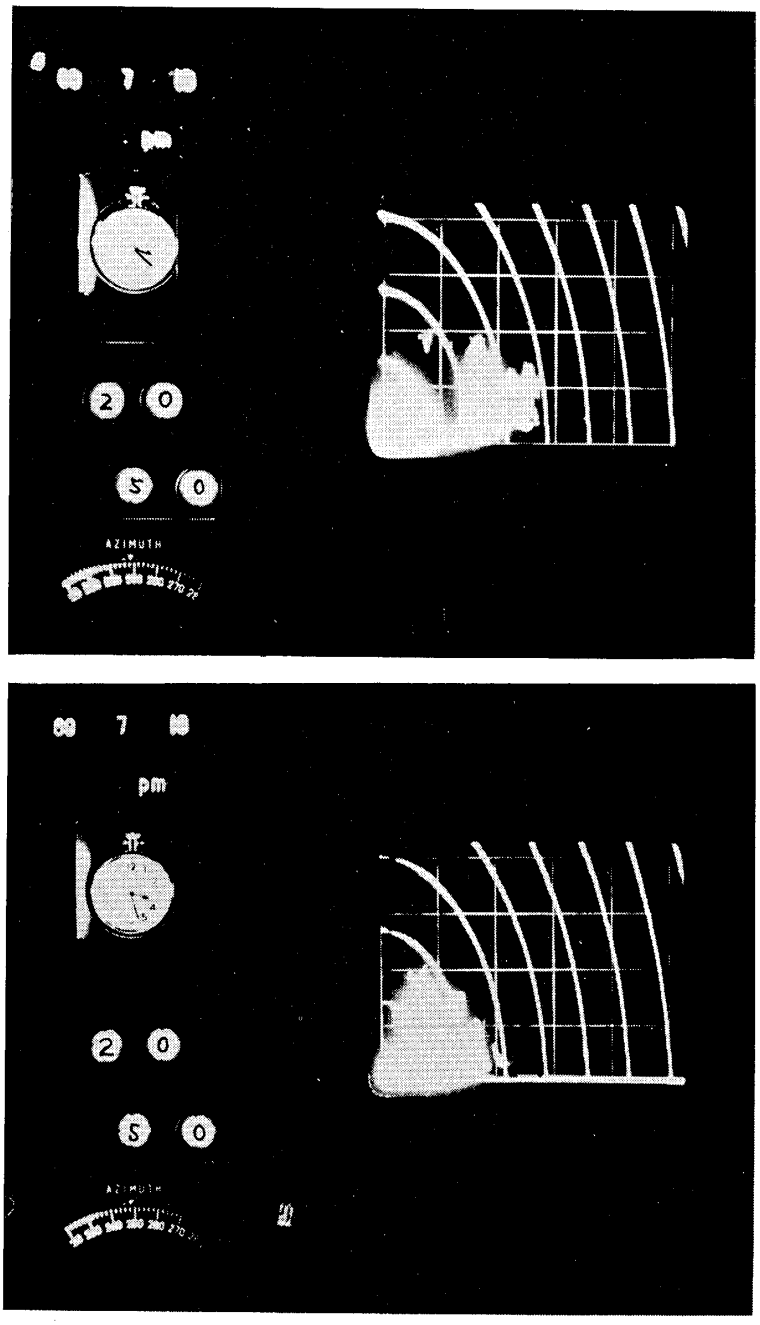

Fig. 12 Another example of coalescence of echoes. The coalesced echo brought the rainfall of Fig. 5 (g).

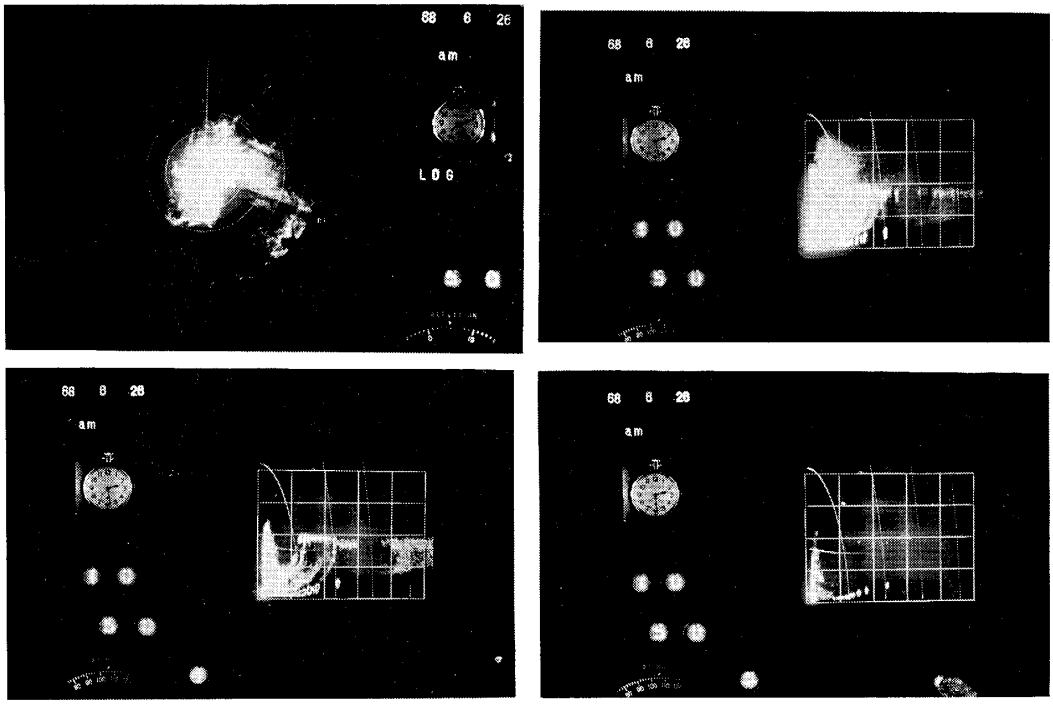

Fig. 13 Example of coexistence of the stratiform rain and the convective rain. The confluent echo comes down to the surface.

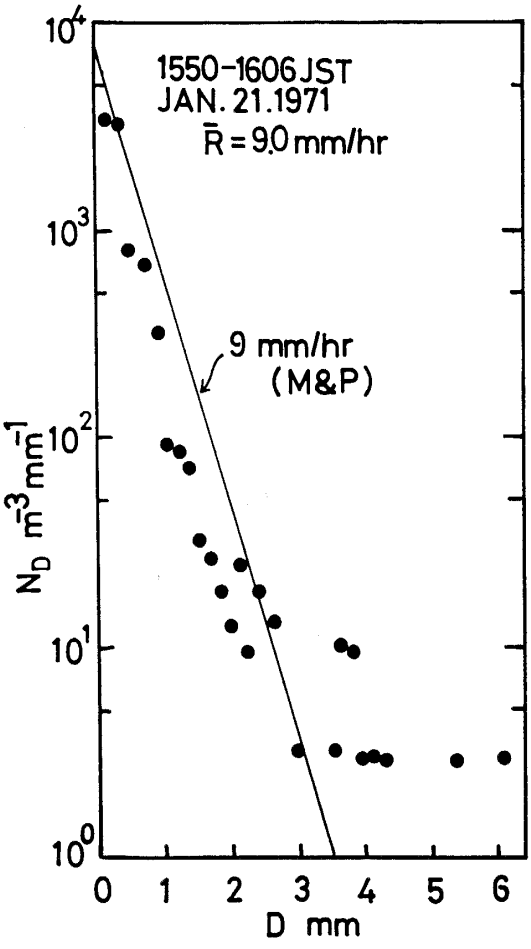

Fig. 14 Average raindrop size distribution from the developed convective rainfall in winter at Hikosan.

radar of Fukuoka Observatory (Fig. 1) revealed that the echo-top height of this precipitation cloud was between 3 to 4 km. It seems to have a a close correspondence to the upper half part of the summer convective clouds. Because, according to soundings at Fukuoka and Kagoshima, the winter temperature profile shows $-10°C$ at 700 mb (near the cloud top) and 10°C at the surface, while the summer temperature profile $-10°C$ at 500 or 400 mb (near the cloud top) and 10°C at 700 mb. As found in the figure, large drops of about 6 mm in diameter were already involved, and the size distributions appeared in remarkable departures from the M–P's, in a similar manner to the case of summer heavy rainfall. Thus, it may be suggested that the coalescence process of raindrops prevailes early in the higher part of the developed convective rain clouds.

On the other hand, the actual distribution at Hitoyoshi have numerous concentrations of smaller drops than 1 mm diameter. This can not be explained by the stationary distribution of Srivastava. The reason may be that drops smaller than 200 μ in diameter was not considered in his numerical experiment. As another reason, the effects of splashing, and the possible existence of orographic warm clouds in the lowest layer which was observed by Blanchard in Hawaii and which had abundant small drops, may be considered.

Part 2 of this report will follow those problems in the present distribution, including the characteristic shape of the instantaneous distributions, by numerical experiments.

5. Conclusion

Simultaneous work of the raindrop sampling and radar observation was made in heavy rainfalls during the last stages of Baiu. A new type of size distributions of raindrops were found in the heavy rainfalls. And explanations and considerations are given in this paper. They are summarized as follows.

(1) The size distributions from the heavy rainfalls reveal remarkable departures from the conventional Marshall-Palmer distributions, as in the profile in which the increased space concentrations of both large and small raindrops and deep dips in the medium size range are seen. They are quite similar to the stationary distributions computed by Srivastava.

(2) And the average size distribution fits well with the parabolic curves on the semi-logarithmic graph paper as shown in Fig. 7. These curves lead to the relationship between the space concentration (N_D) and the diameter (D) of raindrops to the form $N_D=N_0 \exp(-AD^2)$, which is a highly convenient type of equation for calculating various types of rain parameters, similar to the case of $N_D=N_0 \exp(-AD)$ by Marshall and Palmer.

(3) It was noted that a mother rain cloud had some echo characteristics corresponding to the obtained characteristics of size distribution. One of them is the coalescence of the echo cell, as shown in Fig. 11 where two line type convective echoes were united into one echo. The derived rain parameters from

those size distributions appear to be different from those hitherto observed, because of the abundant large drops.

(4) Such combination effects of individual rain clouds are discussed with other examples of coalescence of radar echoes, the existence of orographic warm rain clouds, and the size distributions from the developed winter rain showers. From the results it may be proposed that the combination effect may be also responsible for the size distributions of heavy rainfalls, in addition to the various types of cloud physical effects of drops such as coalescence, spalsh and disintegration on collision.

Acknowledgements

The writer greatly appreciates the advice and guidance given by Prof. Choji Magono, Department of Geophysics of Hokkaido University, throughout the course of this study.

References

1) Atlas, D., 1964: Advances in radar meteorology. Adv. Geophys., **10,** 317–478.
2) Atlas, D., and A.C. Chmela, 1957: Physical synoptic variations of drop-size parameters. Proc. 6th Weather Radar Conf., **4,** 21–29.
3) Best, A.C., 1950: The size distribution of raindrops. Quart. J. Roy. Meteor. Soc., **76,** 16–36.
4) Blanchard, D.C., 1953: Raindrop size distribution in Hawaiian rains. J. Meteor., **10,** 457–473.
5) Blanchard, D.C., and A.T. Spencer, 1970: Experiments on the generation of raindrop-size distributions by drop breakup. J. Atmos. Sci., **27,** 101–108.
6) Dingle, A. N., and K. R. Hardy, 1962: The description of rain by means of sequential raindrop-size distributions. Quart. J. Roy. Meteor. Soc., **88,** 301–314.
7) Fujuwara, M., 1965: Raindrop-size distribution from individual storms. J. Atmos. Sci., **22,** 585–591.
8) Gunn, R., and G. G. Kinzer, 1949: The terminal velocity of fall for water droplets in stagnant air. J. Meteor., **6,** 243–248.
9) Hardy, K. R., 1963: The development of raindrop-size distributions and implications related to the physics of precipitation. J. Atomos. Sci., **20,** 299–312.
10) Jones, D. M. A., 1956: Rainfall drop-size distribution and radar reflectivity. Illinois State Water Survey. Meteor. Lab. Res. Rept., No.6, 20pp. (After Atlas (1964))
11) Joss, J., and A. Waldvogel, 1969: Raindrop size distribution and sampling size errors. J. Atmos. Sci., **26,** 566–569.
12) Ludlum, F. H., 1966: Cumulus and cumulonimbus convection. Tellus, XVIII, 687–698.
13) Marshall, J. S., and W. McK. Palmer, 1948: The distribution of raindrops with size. J. Meteor., **5,** 165–166.
14) Mason, B. J., 1971: The physics of clouds. 671 pp. Clarendor press, Oxford.
15) Mason, B. J., and J. B. Andrews, 1960: Drop-size distributions from various types of rain. Quart. J. Roy. Meteor. Soc., **86,** 346–353.
16) Mason, B. J., and R. Ramanadham, 1954: Modification of the size distribution of falling raindrops by coalescence. Quart. J. Roy. Meteor. Soc., **80,** 388–394.
17) Rigby, J. S., J. S. Marshall and W. Hitschfeld, 1954: The development of the size dis-

tribution of raindrops during their fall. J. Meteor., **11,** 362–372.
18) Sivaramakrishnan, M. V., 1961: Studies of raindrop size characteristics in different types of tropical rain using a simple raindrop recorder. Indian J. Meteor. Geophys., **12,** 189–217. (After Atlas (1964))
19) Srivastava, R. C., 1971: Size distribution of raindrops generated by their breakup and coalescence. J. Atmos. Sci., **28,** 410–415.
20) Takeda, T., 1971: Numerical simulation of a precipitating convective cloud: The formation of a "Long-Lasting" cloud. J. Atmos. Sci., **28,** 350–376.
21) Tatehira, R., 1968: A study of rainband. Geophys. Mag., **34,** 115–138.
22) The Severe Storms Research Group of St. Louis Univ., 1970: F. C. Bate's conceptual thoughts on severe thunderstorms. Bull. Amer. Meteor. Soc., **51,** 481–488.